Impact of Scattering on Communication and Secrecy Performance over Underwater Quantum Links

Qingqing Hu[1], Chen Gong[1], Nuo Huang[1], Jianghua Luo[2,3], and Zhengyuan Xu[1]
[1]Key Laboratory of Wireless-Optical Communications, Chinese Academy of Sciences,
School of Information Science and Technology,
University of Science and Technology of China, Hefei 230027, China.
Email: ruixihu@mail.ustc.edu.cn; cgong821@ustc.edu.cn; huangnuo@ustc.edu.cn; xuzy@ustc.edu.cn.
[2]National Mobile Communications Research Laboratory, Southeast University, Nanjing 210096, China.
[3]School of Physics and Optoelectronic Engineering, Yangtze University, Jingzhou 434023, China.
Email: jhluo@yangtzeu.edu.cn.

2021 13th International Conference on Wireless Communications and Signal Processing (WCSP) | 978-1-6654-0785-4/21/$31.00 ©2021 IEEE | DOI: 10.1109/WCSP52459.2021.9613683

***Abstract*—Considering quantum signal transmission in the underwater links with scattering, we investigate the quantum channel model, the related capacity and secrecy performance. Monte Carlo simulation results demonstrate that the polarization angle change within [-20, 20] degrees accounts for 98%. We propose a quantum channel model for underwater link with scattering and theoretically investigate the capacity, where a larger proportion of scattered photons and a larger variation range of the polarization angle leads to lower quantum classical capacity. We analyze the secret key rate of BB84 protocol under unauthorized receiver attack (URA). The results show the maximum secure transmission distance under the given parameters of seawater decreases from 113 m to 58 m as the probability that the eavesdropper receives scattered photons increases from 0.1% to 10%.**

I. Introduction

Quantum communication, which offers high security based on some principles of quantum mechanics [1], has been considered as a promising solution for cryptography. Furthermore, it is of great significance for future applications in telecommunications, finance and strategy [2].

There are numerous ways to realize quantum bits in quantum communication, and the most common one is to adopt optical signal as carrier. The BB84 protocol is not only the world's first quantum key distribution (QKD) protocol, but also the most practical one being widely adopted [3]. Up to now, massive QKD experiments have been demonstrated worldwide in hundreds of kilometers of optical fibers [4], [5] and free-space air [6], [7]. In recent years, free-space QKD in a water environment has attracted much attention. Decoy-state QKD experiments through 10-m and 30-m underwater channels have been successfully demonstrated [8], [9]. However, one of the challenges for underwater free-space quantum communications is to effectively transmit quantum states in noisy environments. Note that there are a large number of scattering particles in the seawater, leading to the change of the photon transmission direction and the distortion of the polarization state. It significantly limits the maximum achievable rate as well as the communication distance [10]. Researches on simulations and experiments mainly focus on fidelity of photons through underwater channels [11], [12]. The motivation of this paper is to explore the communication performance in terms of channel capacity and analyse the secrecy performance under a special attack, unauthorized receiver attack (URA).

In this paper, we focus on the polarization states of received scattered photons in underwater QKD and a quantum channel model is derived from the polarization angle distribution of received photons. Then, the maximum amount of classical information through the scattering channel is theoretically calculated by using Holevo-Schumacher-Westmoreland (HSW) theorem in [13]. Previous studies mainly analyze two typical active eavesdropping methods, an intercept-resend attack (IRA) and a photon-number-splitting (PNS) attack, in QKD systems [14]. Here, we explore a passive eavesdropping attack, URA, and calculate the secret key rate at different transmission distances, since the scattered photons may be intercepted by passive eavesdroppers due to the change of transmission direction.

This work was supported in part by National Key Research and Development Program of China under Grant 2018YFB1801904, in part by the National Postdoctoral Program for Innovative Talents under Grant BX20190320, in part by the project funded by China Postdoctoral Science Foundation under Grant 2020M671896, in part by Key Program of National Natural Science Foundation of China under Grant 61631018, in part by the National Natural Science Foundation of China under Grant 62171428 and Grant 62101526, in part by Key Research Program of Frontier Sciences of CAS under Grant QYZDY-SSW-JSC003, and in part by the open research fund of National Mobile Communications Research Laboratory Southeast University under Grant 2019D14.

II. Scattering quantum channel modeling

A. Physical channel analysis

Consider an underwater optical wireless communication (OWC) scenario, QKD, as shown in Fig. 1, where the transmitter maps the information bits into several polarization states and sends the polarized photons to the channel. A legitimate receiver is placed in a line-of-sight (LOS) position at the same

depth and makes a measurement on these polarized photons. The photon transmission in the water includes the following cases:

(i) Some of photons arrive directly at the receiver without scattering.

(ii) Due to the massive particles especially the plankton in the seawater, some of photons are scattered and fall outside the receiving aperture, which can be treated as channel loss. An eavesdropper may capture these photons to get the information, threatening the security of communication.

(iii) Some scattered photons are still within the receiving aperture, whose polarization may be changed leading to errors of the received information.

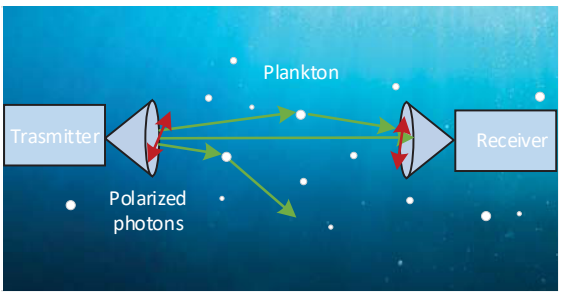

Fig. 1. The propagation of the polarized photons in the water.

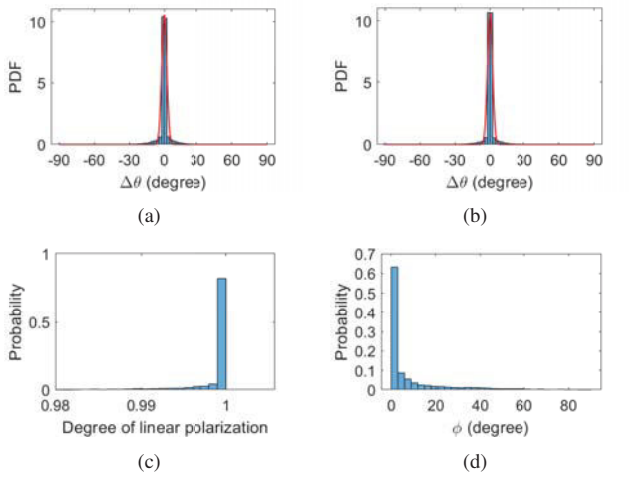

Fig. 2. The PDF of (a) polarization angle change of scattered photons in (a) 1-m link and in (b) 5-m link. The probability distribution of (c) the degree of linear polarization and (d) the angle between the polarization plane and the receiving plane for scattered photons.

To explore the polarization states of scattered photons, we perform channel simulation based on photon tracing, where the Mie scattering of photons by planktonic particles is considered since plankton is widespread in Jerlov type I - III water [15]. The number density and average diameter of planktonic particles in the water are 10^9 /m^3 and 10 um, and the absorption coefficient and the scattering coefficient are 0.0820 /m and 0.0842 /m, close to Jerlov type II water. Assume that the photosensitive area size of the single photon detector (SPD) is $1.3 \times 1.3\text{mm}^2$. 10^8 photons with a wavelength of 520 nm are transmitted and the polarization state of photons can be described by Stokes vectors calculated after each scattering. For more details about the polarization state tracking, we refer the readers to [16].

Fig. 2(a) and Fig. 2(b) shows the probability density distribution (PDF) of the polarization angle change $\Delta\theta$ of the scattered photons in the 1-m link and 5-m link. The cumulative interval is 2 degrees. The proportion of the scattered photon number to the received photon number is 0.03%. It is seen that the dominant polarization angle change lies in the range [-2, 2] degrees and the probability within [-20, 20] degrees reaches 98%. The reason for the small change of photon polarization angle is that most received photons are scattered only once. The PDFs can be fitted by the Von Mises distribution with parameter $\mu = 0$ and $k = 700$, i.e.,

$$f(\theta) = \frac{e^{k\cos(\theta-\mu)}}{2\pi I_0(k)}, \tag{1}$$

where $I_0(*)$ is zero-order modified Bessel function and $\theta \in [-\pi, \pi]$. As seen in Fig. 2(c), the proportion of degree of linear polarization greater than 0.99 is 97.32%. Therefore, it can be considered that the received scattered photons in the aligned receiver are still linearly polarized. The angle ϕ between the polarization plane of scattered photons and the receiving plane is mainly distributed within 20 degrees accounting for 86.45% in Fig. 2(d).

B. Equivalent quantum channel model

Based on the polarization states distribution in the previous section, a equivalent quantum channel model is proposed. The polarization state is one of the quantum states for photons, and the polarization state of a linearly polarized photon with polarization angle θ is denoted as

$$|\psi\rangle = \cos\theta\,|0\rangle + \sin\theta\,|1\rangle = \begin{bmatrix} \cos\theta \\ \sin\theta \end{bmatrix}. \tag{2}$$

The density matrix can be written as

$$\rho = |\psi\rangle\langle\psi| = \begin{bmatrix} \cos^2\theta & \cos\theta\sin\theta \\ \sin\theta\cos\theta & \sin^2\theta \end{bmatrix}. \tag{3}$$

The linearly polarized photons are transmitted through the scattering medium, the received scattered photons maintain a high degree of linear polarization from previous simulation results. Therefore, the quantum channel model can be characterized by the following state evolution matrix, which is a positive definite and trace preserving linear transformation acting on the density matrix space of quantum states,

$$N(\rho) = (1-p)\begin{bmatrix} \cos^2\theta & \cos\theta\sin\theta \\ \sin\theta\cos\theta & \sin^2\theta \end{bmatrix} + p\int_{\theta-\frac{\pi}{2}}^{\theta+\frac{\pi}{2}} f(\theta'-\theta) \times \begin{bmatrix} \cos^2\theta' & \cos\theta'\sin\theta' \\ \sin\theta'\cos\theta' & \sin^2\theta' \end{bmatrix} d\theta', \tag{4}$$

where p is the probability of the received scattered photons; $f(\theta'-\theta)$ is the probability density distribution of change in polarization angle; $(1-p)$ is the probability of the received photons without scattering whose density matrix remains the same. Note that as the period of the polarization direction is π. For instance, 45 degrees and -135 degrees represent the same direction of polarization. The polarization angle of the

scattered photons $\theta' \in [\theta-\pi/2,\ \theta+\pi/2]$. When the polarization angle θ' is uniformly distributed with $f(\theta'-\theta)=1/\pi$, it is equivalent to a typical depolarized channel

$$N(\rho)=(1-p)\,\rho+p\begin{bmatrix}\frac{1}{2} & 0\\ 0 & \frac{1}{2}\end{bmatrix}=(1-p)\,\rho+p\frac{\mathbf{I}}{2}. \tag{5}$$

III. Classical Capacity of Quantum Channels with Joint Measurement Setting

The HSW theorem defines the maximum classical amount of information that can be obtained through a noisy quantum channel when the output is measured by joint measurement setting [13]. The classical capacity of a quantum channel is given by

$$C(N)=\max_{p_i,\ \rho_i}\chi=\max_{p_i,\ \rho_i}\left[S\left(N\left(\sum_i p_i\rho_i\right)\right)-\sum_i p_i S\left(N\left(\rho_i\right)\right)\right], \tag{6}$$

where χ is called Holevo quantity; $S(\rho)=-Tr(\rho\log(\rho))$ is von Neumann entropy which measures the information contained in the quantum system ρ. When transmitting any two linear polarization states, for photons with probability p_1, we have

$$\rho_1=\begin{bmatrix}\cos^2 x & \cos x\sin x\\ \sin x\cos x & \sin^2 x\end{bmatrix}, \tag{7}$$

and for photons with probability $p_2=1-p_1$, we have

$$\rho_2=\begin{bmatrix}\cos^2(x+y) & \cos(x+y)\sin(x+y)\\ \sin(x+y)\cos(x+y) & \sin^2(x+y)\end{bmatrix}. \tag{8}$$

The density matrix at the receiver is

$$\begin{aligned}&N\left(\sum_i p_i\rho_i\right)=p_1(1-p)\begin{bmatrix}\cos^2 x & \sin(2x)/2\\ \sin(2x)/2 & \sin^2 x\end{bmatrix}\\ &+p_1 p\int_{x-\frac{\pi}{2}}^{x+\frac{\pi}{2}} f(\theta'-x)\begin{bmatrix}\cos^2\theta' & \sin(2\theta')/2\\ \sin(2\theta')/2 & \sin^2\theta'\end{bmatrix}d\theta'\\ &+(1-p_1)(1-p)\begin{bmatrix}\cos^2(x+y) & \sin(2x+2y)/2\\ \sin(2x+2y)/2 & \sin^2(x+y)\end{bmatrix}\\ &+(1-p_1)\,p\int_{x+y-\frac{\pi}{2}}^{x+y+\frac{\pi}{2}} f(\theta'-x-y)\begin{bmatrix}\cos^2\theta' & \frac{\sin(2\theta')}{2}\\ \frac{\sin(2\theta')}{2} & \sin^2\theta'\end{bmatrix}d\theta'\end{aligned} \tag{9}$$

For simplicity of notation, we define variables a and b to replace the integral term, and Eq. (9) can be rewritten as

$$N\left(\sum_i p_i\rho_i\right)=\begin{bmatrix}n_1 & n_2\\ n_2 & 1-n_1\end{bmatrix}, \tag{10}$$

where

$$\begin{aligned}&n_1=p_1 p\left(\left(a-\tfrac{1}{2}\right)\cos(2x)-b\sin(2x)+\tfrac{1}{2}\right)\\ &p_1(1-p)\cos^2 x+(1-p_1)(1-p)\cos^2(x+y)+(1-p_1)\\ &\times p\left(\left(a-\tfrac{1}{2}\right)\cos(2x+2y)-b\sin(2x+2y)+\tfrac{1}{2}\right),\end{aligned} \tag{11}$$

$$\begin{aligned}&n_2=p_1 p\left(b\cos(2x)+\left(a-\tfrac{1}{2}\right)\sin(2x)\right)\\ &+\tfrac{1}{2}p_1(1-p)\sin(2x)+\tfrac{1}{2}(1-p_1)(1-p)\sin(2x+2y)\\ &+(1-p_1)\times p\left(b\cos(2x+2y)+\left(a-\tfrac{1}{2}\right)\sin(2x+2y)\right),\end{aligned} \tag{12}$$

$$\int_{-\frac{\pi}{2}}^{\frac{\pi}{2}} f(\theta')\times\begin{bmatrix}\cos^2\theta' & \cos\theta'\sin\theta'\\ \sin\theta'\cos\theta' & \sin^2\theta'\end{bmatrix}d\theta'\triangleq\begin{bmatrix}a & b\\ b & 1-a\end{bmatrix}. \tag{13}$$

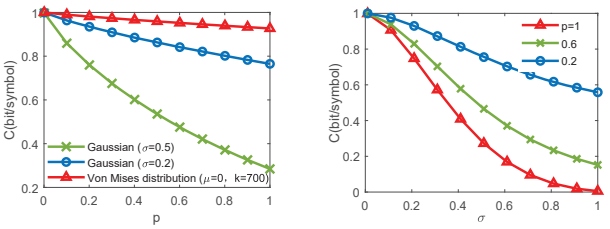

(a) (b)

Fig. 3. Classical capacity versus (a) the probability of received scattered photons and (b) the standard deviation of truncated Gaussian distribution of polarization angle.

Then, the classical capacity can be obtained as

$$\begin{aligned}&C(N)\\ &=\max_{p_i,\ \rho_i}\left(\begin{array}{l}H_2\left(\frac{1}{2}+\frac{1}{2}\sqrt{\left[\begin{array}{l}\left(4p_1\sin^2 y\,(p_1-1)+1\right)\times\\ \left((2p-2pa-1)^2+4p^2b^2\right)\end{array}\right]}\right)\\ -H_2\left(\frac{1}{2}+\frac{1}{2}\sqrt{(2p-2pa-1)^2+4p^2b^2}\right)\end{array}\right),\end{aligned} \tag{14}$$

where $H_2(x)=-x\log_2 x-(1-x)\log_2(1-x)$ is binary entropy function. Note that when two orthogonal states with probability $\frac{1}{2}$ are transmitted ($y=\frac{\pi}{2}$ and $p_1=\frac{1}{2}$), $4{p_1}^2\sin^2 y-4p_1\sin^2 y+1=0$ and the first term in Eq. (14) has a maximum value of 1. Then, the maximum capacity is given by

$$C(N)=1-H_2\left(\frac{1}{2}+\frac{1}{2}\sqrt{(2p-2pa-1)^2+4p^2b^2}\right). \tag{15}$$

The capacity are related to the probability distribution of polarization angle change and the probability of receiving the scattered photons.

We calculate variables a and b according to the Eq. (13) when the polarization angle change $(\theta'-\theta)\in[-\pi/2,\pi/2]$ satisfies truncated Gaussian distribution or Von Mises distribution in Fig. 2(a). Given a and b, the classical capacity of quantum channels is calculated under different probability of received scattered photons p as shown in Fig. 3(a). It is seen that the capacity decreases as the proportion of scattered photons increases. For Von Mises distribution distribution in Fig. 2(a), when received photons are all scattered photons ($p=1$), the channel capacity decreases slightly to 0.93. From Fig. 3(b), larger standard deviation σ of the truncated Gaussian distribution of polarization angle leads to lower channel capacity. When $p=1$ and $\sigma=1$, the capacity decreases to 0.005.

IV. Secret Key Rate of BB84 Protocol Under an URA

In BB84 protocol, Alice and Bob exchange classical sequences encoded in non-orthogonal quantum states over the quantum channel to impede eavesdropping the quantum states without error. Since Bob measures the output independently, the capacity is equal to the maximal mutual information, which is not greater than the classical capacity with joint measurement setting calculated in Section III [17], [18].

Fig. 4 shows the forward transition probability of BB84 protocol after independent measurement. Assume a1 to a4 are

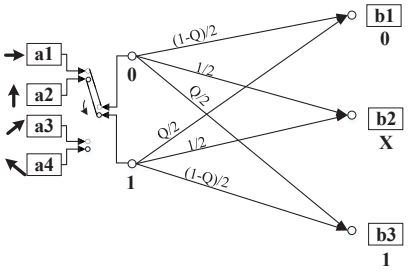

Fig. 4. Forward transition probability.

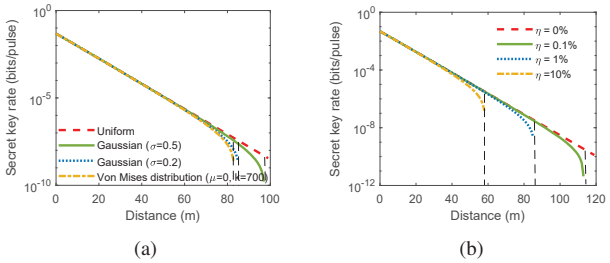

Fig. 5. (a) The relation of secret key rate and distance for different distributions of polarization angle (receiving probability of Eve=1%). (b) The relation of secret key rate and distance under different receiving probabilities of Eve (truncated Gaussian distribution ($\sigma = 0.2$)).

transmitted with respective probabilities of q_1 to q_4. When $q_1 = q_2 = q_3 = q_4 = 1/4$, the maximum mutual information is

$$\begin{aligned}\max_{q_i} I(A;B) &= 1 + \tfrac{1}{2}(1-Q)\log\left(\tfrac{1}{2}(1-Q)\right) + \tfrac{1}{2}Q\log\left(\tfrac{1}{2}Q\right)\\ &= \tfrac{1}{2}(1-H_2(Q)) = \tfrac{1}{2}(1-H_2(p-pa)),\end{aligned} \tag{16}$$

where Q is the error probability due to scattering, given by

$$Q = \int_{\theta_t-\frac{\pi}{2}}^{\theta_t+\frac{\pi}{2}} f(\theta_r-\theta_t)\cos^2\left(\theta_r-\left(\theta_t+\frac{\pi}{2}\right)\right)d\theta_r = p(1-a), \tag{17}$$

where θ_t is the polarization angle of transmitted photons; θ_r is the polarization angle of received photons; $f(\theta_r-\theta_t)$ is the probability distribution of change in the polarization angle; p is the probability of received scattered photons; and a is defined in Eq. (13).

Since the scattering will cause the photon transmission direction change, and the scattered photons may be intercepted by passive eavesdroppers, non-ideal single photon source will lead to information leakage. However, it is difficult for both the transmitter and the receiver to detect whether there is an eavesdropper stealing the scattered photons. It is necessary to investigate the secrecy performance if there exists an URA. Assume that Alice sends an n-photon pulse, where the photon number n follows the Poisson distribution with mean u. The transmission rates due to the channel absorption and scattering are $t_a = e^{-\mu_a L}$ and $t_s = e^{-\mu_s L}$, respectively, where μ_a is the absorption coefficient, μ_s is the scattering coefficient and L is the transmission distance. The total transmission rate is $t = t_a t_s$. When Alice sends the pulse with n photons, due to the absorption and scattering, the probability of at least one photon received by Bob is $1-(1-t)^n$ [19]. Bob's average count rate per pulse is $q_u = \sum_{n=0}^{\infty}\frac{u^n}{n!}e^{-u}\times(1-(1-t)^n) = 1-e^{-ut}$. Here, we mainly study the effect of scattered photons and dark count is not taken into account. The average mutual information per pulse between Alice and Bob can be expressed as

$$I(A;B) = \frac{1}{2}q_u \times (1-H_2(Q)). \tag{18}$$

When Alice sends the multiple-photon pulse and Bob's detector responds, Eve may capture the scattered photons to eavesdrop useful information. Assuming the worst case, Bob's detector also responds when Eve receives at least one scattered photon. Eves average count rate per pulse is $q_m = \sum_{n=2}^{\infty}\frac{u^n}{n!}e^{-u}\times\left(1-(1-t')^n\right) = 1-e^{-ut'}-ut'e^{-u}$, where $t' = \eta t_a(1-t_s)$ and η is the probability of residual scattered photons received by Eve. The mutual information between Alice and Eve is

$$I(A;E) = \frac{1}{2}q_m \times (1-H_2(Q')), \tag{19}$$

where $Q' = \int_{\theta_t-\frac{\pi}{2}}^{\theta_t+\frac{\pi}{2}} f(\theta_{r'}-\theta_t)\cos^2\left(\theta_{r'}-\left(\theta_t+\frac{\pi}{2}\right)\right)d\theta_{r'}$ is the error probability due to the scattered photons received by Eve. The secret key rate in the presence of an unauthorized receiver attack is

$$R_s = \max\{I(A;B) - I(A;E),\ 0\}. \tag{20}$$

Let $\mu_a = 0.0820$, $\mu_s = 0.0842$, close to Jerlov type II water. u= 0.1. Fig. 5(a) shows the secret key rate varies with distance when probability of receiving scattered photons of Eve=1%. As photons travel longer distances, more photons are scattered and more information is leaked. Therefore, the secret key rate is decreasing gradually with the distance. Assume that the distribution for polarization angle satisfies truncated Gaussian distributions (the standard deviation $\sigma = 0.2, 0.5$) and the Von Mises distribution from simulation results in Section II-A, respectively. It is seen that the secret key rate of the same transmission distance decreases as the variation range of polarization angle decreases. The reason is that the scattered photons received by Eve contain more information for smaller change of the polarization angle, leading to lower secret key rate. Fig. 5(b) shows the secret key rate varies with distance under different receiving probabilities η of Eve. When the probability that Eve receives scattered photons increases from 0.1% to 10%, the maximum secure transmission distance under the given parameters of seawater decreases from 113 m to 58 m. As the receiving probability η decreases, both the secure transmission distance and secret key rate are growing steadily. There are two special cases, polarization angle change satisfies the uniform distribution in Fig. 5(a) or receiving probability of Eve $\eta = 0\%$ in Fig. 5(b), corresponding to the zero mutual information of Eve.

V. Conclusion

In this work, an underwater quantum channel with scattering is investigated. The Monte Carlo simulations show that the received scattered photons still maintain a high degree of linear

polarization and the probability within [-20, 20] degrees accounts for 98%. The quantum classical capacity is analytically derived based on the proposed quantum channel model, where a larger variation of polarization angle and a larger probability of scattered photons will lead to a lower capacity. The secret key rate of BB84 protocol under unauthorized receiver attack is deduced theoretically in the scattering link, and the results show that the maximum secure transmission distance under the given parameters of seawater decreases from 113 m to 58 m as the probability that the eavesdropper receives scattered photons increases from 0.1% to 10%.

REFERENCES

[1] H. Zhang, Z. Ji, H. Wang, and W. Wu, "Survey on quantum information security," *China Communications*, vol. 16, no. 10, pp. 1–36, 2019.

[2] M. Sasaki, "Quantum key distribution and its applications," *IEEE Security & Privacy*, vol. 16, no. 5, pp. 42–48, 2018.

[3] W.-Y. Hwang, "Quantum key distribution with high loss: toward global secure communication," *Physical Review Letters*, vol. 91, no. 5, p. 057901, 2003.

[4] T. Länger and G. Lenhart, "Standardization of quantum key distribution and the etsi standardization initiative isg-qkd," *New Journal of Physics*, vol. 11, no. 5, p. 055051, 2009.

[5] T. Chapuran, P. Toliver, N. Peters, J. Jackel, M. Goodman, R. Runser, S. McNown, N. Dallmann, R. Hughes, K. McCabe *et al.*, "Optical networking for quantum key distribution and quantum communications," *New Journal of Physics*, vol. 11, no. 10, p. 105001, 2009.

[6] L. Bacsardi, "On the way to quantum-based satellite communication," *IEEE Communications Magazine*, vol. 51, no. 8, pp. 50–55, 2013.

[7] S. Nauerth, F. Moll, M. Rau, C. Fuchs, J. Horwath, S. Frick, and H. Weinfurter, "Air-to-ground quantum communication," *Nature Photonics*, vol. 7, no. 5, pp. 382–386, 2013.

[8] Z. Feng, S. Li, and Z. Xu, "Experimental underwater quantum key distribution," *Optics Express*, vol. 29, no. 6, pp. 8725–8736, 2021.

[9] C.-Q. Hu, Z.-Q. Yan, J. Gao, Z.-M. Li, H. Zhou, J.-P. Dou, and X.-M. Jin, "Decoy-state quantum key distribution over a long-distance high-loss air-water channel," *Physical Review Applied*, vol. 15, no. 2, p. 024060, 2021.

[10] H. Ding, G. Chen, A. K. Majumdar, B. M. Sadler, and Z. Xu, "Modeling of non-line-of-sight ultraviolet scattering channels for communication," *IEEE Journal on Selected Areas in Communications*, vol. 27, no. 9, pp. 1535–1544, 2009.

[11] P. Shi, S.-C. Zhao, Y.-J. Gu, and W.-D. Li, "Channel analysis for single photon underwater free space quantum key distribution," *JOSA A*, vol. 32, no. 3, pp. 349–356, 2015.

[12] L. Ji, J. Gao, A.-L. Yang, Z. Feng, X.-F. Lin, Z.-G. Li, and X.-M. Jin, "Towards quantum communications in free-space seawater," *Optics Express*, vol. 25, no. 17, pp. 19 795–19 806, 2017.

[13] L. Gyongyosi, S. Imre, and H. V. Nguyen, "A survey on quantum channel capacities," *IEEE Communications Surveys & Tutorials*, vol. 20, no. 2, pp. 1149–1205, 2018.

[14] S. Sajeed, I. Radchenko, S. Kaiser, J.-P. Bourgoin, A. Pappa, L. Monat, M. Legré, and V. Makarov, "Attacks exploiting deviation of mean photon number in quantum key distribution and coin tossing," *Physical Review A*, vol. 91, no. 3, p. 032326, 2015.

[15] J. R. V. Zaneveld, "Light and water: Radiative transfer in natural waters," 1995.

[16] J. C. Ramella-Roman, S. A. Prahl, and S. L. Jacques, "Three monte carlo programs of polarized light transport into scattering media: part i," *Optics Express*, vol. 13, no. 12, pp. 4420–4438, 2005.

[17] C. H. Bennett and P. W. Shor, "Quantum information theory," *IEEE Transactions on Information Theory*, vol. 44, no. 6, pp. 2724–2742, 1998.

[18] C. A. Fuchs, "Nonorthogonal quantum states maximize classical information capacity," *Physical Review Letters*, vol. 79, no. 6, p. 1162, 1997.

[19] Z. Chang-Hua, P. Chang-Xing, Q. Dong-Xiao, G. Jing-Liang, C. Nan, and Y. Yun-Hui, "A new quantum key distribution scheme based on frequency and time coding," *Chinese Physics Letters*, vol. 27, no. 9, p. 090301, 2010.